THE JOURNAL OF BIOLOGICAL CHEMISTRY Vol. 278, No. 12, Issue of March 21, pp. 10649–10656, 2003

Printed in U.S.A.

Functional Expression and Characterization of an Archaeal Aquaporin

AqpM FROM *METHANOTHERMOBACTER MARBURGENSIS**

Received for publication, December 5, 2002, and in revised form, January 3, 2003
Published, JBC Papers in Press, January 7, 2003, DOI 10.1074/jbc.M212418200

David Kozono‡§, Xiaodong Ding§¶, Ikuko Iwasaki¶, Xianying Meng‖, Yoichi Kamagata‖, Peter Agre‡, and Yoshichika Kitagawa¶‡‡**

From the ‡Departments of Biological Chemistry and Medicine, The Johns Hopkins University School of Medicine, Baltimore, Maryland 21205-2185, ¶Biotechnology Institute, Akita Prefectural University, Ogata, 010-0444, and ‖Microbial and Genetic Resources Research Group, Research Institute of Biological Resources, National Institute of Advanced Industrial Science and Technology, Central 6, Higashi 1-1-1, Tsukuba, Ibaraki 305-8566, Japan

Researchers have described aquaporin water channels from diverse eubacterial and eukaryotic species but not from the third division of life, Archaea. *Methanothermobacter marburgensis* is a methanogenic archaeon that thrives under anaerobic conditions at 65 °C. After transfer to hypertonic media, *M. marburgensis* sustained cytoplasmic shrinkage that could be prevented with $HgCl_2$. We amplified *aqpM* by PCR from *M. marburgensis* DNA. Like known aquaporins, the open reading frame of *aqpM* encodes two tandem repeats each containing three membrane-spanning domains and a pore-forming loop with the signature motif Asn-Pro-Ala (NPA). Unlike other known homologs, the putative Hg^{2+}-sensitive cysteine was found proximal to the first NPA motif in AqpM, rather than the second. Moreover, amino acids distinguishing water-selective homologs from glycerol-transporting homologs were not conserved in AqpM. A fusion protein, 10-His-AqpM, was expressed and purified from *Escherichia coli*. AqpM reconstituted into proteoliposomes was shown by stopped-flow light scattering assays to have elevated osmotic water permeability (P_f = 57 $\mu m \cdot s^{-1}$ *versus* 12 $\mu m \cdot s^{-1}$ of control liposomes) that was reversibly inhibited with $HgCl_2$. Transient, initial glycerol permeability was also detected. AqpM remained functional after incubations at temperatures above 80 °C and formed SDS-stable tetramers. Our studies of archaeal AqpM demonstrate the ubiquity of aquaporins in nature and provide new insight into protein structure and transport selectivity.

To withstand environmental and physiological stresses, organisms must be able to rapidly absorb and release water. Facilitated transport of water across cell membranes must be highly selective to prevent uncontrolled movement of other solutes, protons, and ions. Discovery of the aquaporins provided a molecular explanation to these processes (2). More than 200 aquaporins have now been identified, and their presence has been established in most forms of life (3). No aquaporin from Archaea has yet been characterized, although functional roles for a water channel protein have been predicted in these organisms (4).

Two major protein family subsets are presently recognized, water-selective channels (aquaporins) and glycerol-transporting homologs with varying water permeabilities (aquaglyceroporins). The permeation selectivity of new members of the protein family may be predicted by a small number of conserved residues (5, 6). Several prokaryotic aquaporins and aquaglyceroporins are known. The bacterial water channel, AqpZ, was first identified in *Escherichia coli* (7, 8). Movement of water across the bacterial plasma membrane may be part of the osmoregulatory response by which microorganisms adjust cell turgor (9), although the regulation and physiological role of AqpZ are being reassessed (10). AqpZ is a highly stable tetramer with negligible permeability to glycerol. In contrast, the glycerol permeability of the glycerol facilitator (GlpF) from *E. coli* has long been recognized (11). GlpF has relatively limited water permeability (12), and the tetrameric form has reduced stability in some detergents (13). Atomic resolution structures have been solved for GlpF (14) as well as human and bovine AQP1[1] (15–17). These have elucidated differential specificities and functional mechanisms of the two sequence-related proteins.

Archaea and certain other microorganisms are able to withstand exceptional challenges in maintaining water balance as they thrive in extreme environments including saturated salt solutions, extreme pH, and temperatures up to 130 °C (18). We recently recognized the DNA sequence of AqpM, a candidate aquaporin or aquaglyceroporin in the genome of a methanogenic thermophilic archaeon, *Methanothermobacter marburgensis*[2] (19). Here we investigate water permeability in living cells and report the purification, functional reconstitution, and characterization of AqpM.

* This work was supported by a grant-in-aid (to Y. K.) from the Japanese Society for Promotion of Science Postdoctoral Fellowship P00208 for foreign researcher and grants from the National Institutes of Health and the Human Frontier Science Program. The costs of publication of this article were defrayed in part by the payment of page charges. This article must therefore be hereby marked "*advertisement*" in accordance with 18 U.S.C. Section 1734 solely to indicate this fact.

§ Both authors contributed equally to this work.

** To whom correspondence may be addressed: Dept. Biological Chemistry, The Johns Hopkins School of Medicine, 725 N. Wolfe St., Baltimore, MD 21212-2185. Tel.: 410-955-7049; Fax: 410-955-3149; E-mail: pagre@jhmi.edu.

‡‡ To whom correspondence may be addressed: Biotechnology Institute, Akita Prefectural University, Ogata, 010-0044, Japan. Tel.: 81-185-45-3930; Fax: 81-185-45-2678; E-mail: kitagawa@agri.akita-pu.ac.jp.

[1] The abbreviations used are: AQP, aquaporin; GlpF, glycerol facilitator; MIP, major intrinsic protein; MOPS, 3-(*N*-morpholino)propanesulfonic acid; OG, *n*-octyl-β-D-glucopyranoside; DM, *n*-dodecyl-β-D-maltopyranoside; NTA, nitrilotriacetic acid; BSA, bovine serum albumin; TM, transmembrane.

[2] *Methanobacterium thermoautotrophicum* strain Marburg has been redesignated *Methanothermobacter marburgensis* Marburg (1).

EXPERIMENTAL PROCEDURES

Materials—Microbial growth media components were from Difco or Bio 101, Inc. (Vista, CA). Restriction enzymes were from Takara Biomedicals or New England Biolabs. *n*-Octyl-β-D-glucopyranoside (OG) and *n*-dodecyl-β-D-maltoside (DM) were purchased from Calbiochem. Ni-NTA-agarose was from Qiagen. *E. coli* total lipid extract, acetone/ether preparation, was from Avanti Polar Lipids. Other reagents were from Sigma or Wako Chemicals.

Transmission Electron Microscopy—M. marburgensis cells were grown at 65 °C in 100 ml of medium as reported (20) until exponential phase (A_{600} = 0.8). Culture aliquots of 10 μl were transferred to three tubes. $HgCl_2$ was added to one tube to a final concentration of 1 mM and gently shaken at room temperature for 30 min. The cells of the three tubes were pelleted rapidly and resuspended in 1.0 ml of fresh media at room temperature. A 2.5-μl drop of the cell suspension was placed directly on a copper grid coated with a thin carbon film, upon which osmotic challenges were performed. Osmotic up-shocks were induced by rapidly mixing 2.5 μl of medium containing 2 M mannitol (final mannitol concentration was 1 M after mixing). After 10 s, the cells were harvested by centrifugation and sandwiched between 2 copper discs of 3 mm diameter, and then immediately plunged into propane slush at liquid nitrogen temperature. The copper discs were transferred to liquid nitrogen and separated to expose cells. The frozen samples were freeze-substituted in acetone containing 2% osmium tetroxide at −80 °C for 2 days, then at −20 °C for 2 h, and 4 °C for 2 h. The samples were rinsed with fresh absolute acetone and embedded in Spurr resin (Quetol 653). Thin sections (70–80 nm) were gathered on copper grids covered with Formvar, double-stained with uranyl acetate and lead citrate, and examined under a transmission electron microscope (Hitachi H-7000).

Expression Plasmids and Strains—The plasmid pTrc10HisAqpZ (8) was digested with *Eco*RI and *Sal*I, and *aqpM* from *M. marburgensis* (19) was inserted in place of AqpZ. The resulting construct, pTrc10HisAqpM (encoding 10-His-AqpM) contains the sequence of commercially available pTrc99A (Amersham Biosciences) with the sequence *Nco*I-*Sal*I, replaced by insertion of the sequence for a 10× His tag (MGHHHHHHHHHHSSIEGRHEF) followed by the coding sequence for AqpM. *E. coli* strain BL21-CodonPlus(DE3)-RIL (Stratagene) was transformed with the expression construct. *E. coli* strain XL1Blue (Stratagene) transformed with pTrc10HisAqpZ was used for 10-His-AqpZ expression, and XL1Blue transformed with pTrc10HisGlpF (13) was used for 10-His-GlpF expression. For heterologous expression of rat AQP4, the plasmid pYES2 10xHis-hAQP1 (21) was digested with *Eco*RI and *Xba*I, and the gene encoding full-length rat AQP4 was inserted in place of hAQP1. A *pep4*-deficient strain of *Saccharomyces cerevisiae* with lowered proteolytic activity was transformed with the expression construct.

Expression of 10-His-tagged Aquaporins and Preparation of Membrane Fractions—For expression of bacterial aquaporins, 1-liter cultures of *E. coli* harboring the pTrc10HisAqpM, pTrc10HisAqpZ, or pTrc10HisGlpF construct were propagated in Luria broth containing 50 μg/ml ampicillin at 37 °C to an optical density of about 1.5. Expression of recombinant protein was induced by the addition of 1 mM isopropyl-β-D-thiogalactoside and incubation at 37 °C for 2 h. Harvested cells were resuspended in 1:100 culture volume of ice-cold lysis buffer (100 mM K_2HPO_4, 1 mM $MgSO_4$, 0.4 mg/ml lysozyme, 0.1 mg/ml DNase I, and 1 mM phenylmethylsulfonyl fluoride) and subjected to three French press cycles (18,000 pounds/square inch) at 4 °C. For heterologous expression of rat AQP4, a 1-liter culture of *pep4 S. cerevisiae* harboring the pYES2–10xHis-rAQP4 construct was propagated in Ura- media (27 g of Dropout Base + 0.77 g of Complete supplement mixture minus uracil) at 30 °C to an optical density of about 1.0 and then harvested and used to inoculate 6 liters of YP-Gal (2% Bactopeptone, 1% yeast extract, 2% galactose). This culture was propagated at 30 °C for about 18 h to an optical density of around 6–7. Harvested cells were resuspended in 1/15 culture volume of 100 mM K_2HPO_4 and subjected to two French press cycles (20,000 pounds/square inch) at 4 °C. For all protein preparations, unbroken cells and debris were separated from the cell lysate by a 10-min centrifugation at 6,000 × *g* and discarded. The membrane fraction was recovered from the supernatant by a 60-min centrifugation at 200,000 × *g*.

Purification of His-tagged Aquaporins—The detergent OG was used for AqpM, GlpF, and rAQP4 purification; the detergent DM was used for AqpZ purification. The membrane fraction was resuspended to the volume used for French press with solubilization buffer (3% detergent in 100 mM K_2HPO_4, 10% (v/v) glycerol, 5 mM β-mercaptoethanol, and 200 mM NaCl, pH 8.0) and incubated on ice for 1 h. Insoluble material was pelleted by a 45-min centrifugation at 200,000 × *g* and discarded.

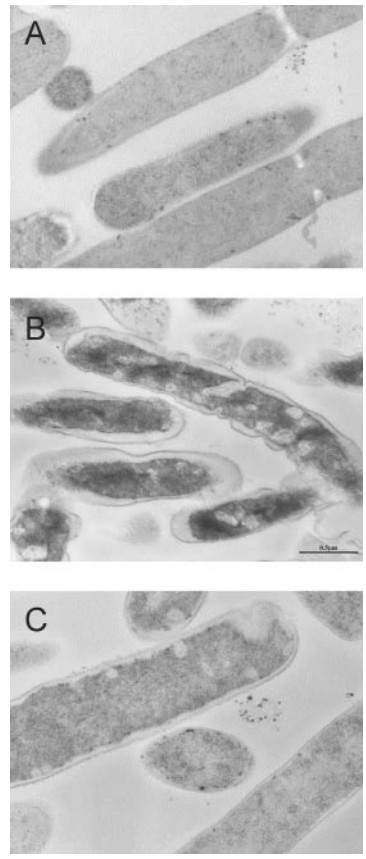

FIG. 1. **Transmission electron micrographs of *M. marburgensis* cells.** *A*, control cells without any treatment (×39,000). *B*, cells exposed to a 1 M mannitol hyperosmotic shock for 10 s (×78,000). *C*, cells pretreated with 1 mM $HgCl_2$ for 30 min and then exposed to hyperosmotic shock (×52,000).

The soluble fraction was mixed with 1–2 ml of prewashed Ni-NTA-agarose beads and incubated with gentle agitation at 4 °C overnight. The beads were then packed in a glass/plastic Econo column (Bio-Rad) and washed with 100 bead volumes of wash buffer (2% detergent, 100 mM K_2HPO_4, 10% glycerol, 5 mM β-mercaptoethanol, 200 mM NaCl, and 100 mM imidazole, pH 7.0) to remove nonspecifically bound materials. Ni-NTA-agarose-bound material was eluted with 0.5–1-ml amounts of elution buffer (2% detergent, 100 mM K_2HPO_4, 10% glycerol, 5 mM β-mercaptoethanol, 200 mM NaCl, and 1 M imidazole, pH 7.0). Protein concentrations were measured by the Schaffner-Weissman filter protein assay method (22) with BSA as a standard.

Sedimentation Analysis—Velocity sedimentation analysis was used to determine the oligomeric structure of purified protein. Detergent-solubilized material (2–10 μg of purified protein in a 200-μl sample volume) was layered on top of a 4-ml continuous sucrose gradient (20 mM Tris·HCl, 5 mM EDTA, 3% OG, 1 mM NaN_3, and 5–20% sucrose, pH 8.0) and centrifuged at 140,000 × *g* for 18 h in a KNOTRON swing-out TST60.4 rotor at 20 °C. Up to 20 fractions were collected and analyzed by SDS-PAGE to determine the migration of the protein. Pure protein was detected by Coomassie Brilliant Blue staining. The sedimentation coefficient ($s_{20,w}$) of each species was determined by interpolation of the relative migration *versus* sedimentation coefficient linear function for the following standards: cytochrome *c* (1.8), carbonic anhydrase (2.9), BSA (4.3), β-amylase (8.9), and catalase (11.2).

Functional Reconstitution—Purified AqpM protein was reconstituted into proteoliposomes by the dilution method, because the dialysis method yielded non-functional proteoliposomes. *E. coli* total lipid extract (acetone/ether preparation, Avanti Polar Lipids) was hydrated in 2 mM β-mercaptoethanol to a final concentration of 50 mg/ml, incubated at room temperature for 1 h, divided into aliquots, and frozen at −80 °C. Before use, lipids were diluted in a borosilicate tube (16 × 125 mm) under a nitrogen/argon atmosphere to a final concentration of 45 mg/ml in 50 mM MOPS-Na, pH 7.5, and pulsed in a bath sonicator until a clear suspension was obtained. A reconstitution mixture was prepared in a glass tube at room temperature by sequentially adding (to final concentrations) 100 mM MOPS-Na, pH 7.5, 1.25% (w/v) OG, 133 μg/ml purified

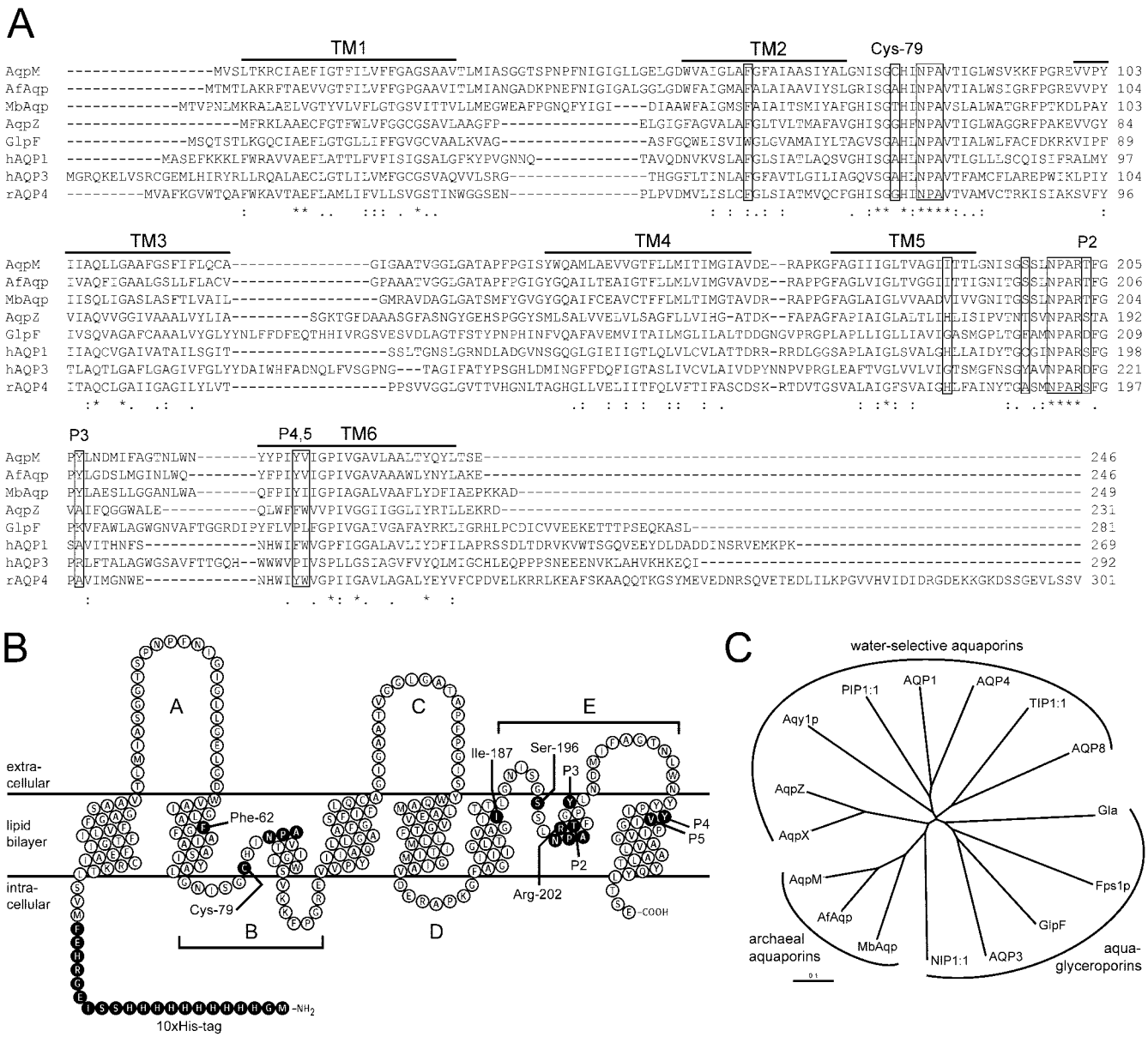

FIG. 2. **Comparative alignment, predicted membrane topology, and phylogeny of AqpM.** *A*, multiple sequence alignment was performed with ClustalX 1.81, with the following GenBank™ accession numbers: AqpM (AB055880), *A. fulgidus* aquaporin homolog "AfAqp" (NP_070255), *M. barkeri* aquaporin homolog "MbAqp" (ZP_00077803), *E. coli* AqpZ (AAC43518), and GlpF (NP_418362), human aquaporin-1 (NP_000376), human aquaporin-3 (NP_004916), and rat aquaporin-4 (NP_036957). *Single bold surface lines* indicate the six transmembrane domains, *TM1–TM6*. *Asterisks*, *colons*, and *periods* indicate perfectly, highly, and moderately conserved amino acid sites, respectively. *B*, predicted membrane topology of 10-His-AqpM. The putative transmembrane domains were assigned by hydrophobicity analysis and manually threading the sequence of AqpM through the x-ray crystal structure of *E. coli* GlpF (Protein Data Bank code 1FX8). The topology map was drawn with TeXtopo. *C*, an unrooted phylogenetic tree of aquaporins was reconstructed with the neighbor-joining method of inference. Proteins previously determined experimentally to be aquaglyceroporins or water-selective aquaporins are indicated.

protein, and 10 mg/ml sonicated lipids (protein/lipid = 1:75). The reconstitution mixture was injected into 25 volumes of assay buffer under constant stirring to dilute the detergent. Liposomes were harvested by centrifugation (45 min at 140,000 × *g*) and resuspended into assay buffer (50 mM MOPS and 150 mM N-methyl-D-glucamine, pH 7.50, with HCl). Protein content was measured as described (22) with BSA as a standard.

Membrane Permeability Measurements—The osmotic behaviors of reconstituted proteoliposomes and control liposomes were analyzed by following the light scattering of the preparation in a stopped-flow apparatus with a dead time of ≤1 ms (SF-2001; KinTek Instruments, University Park, PA). Water permeability was measured by rapidly mixing 100 μl of a proteoliposome suspension (1 μg of protein and 75 μg of *E. coli* polar phospholipids) in assay buffer (see above) with a similar volume of hyperosmolar solution (assay buffer with 570 mOSM sucrose added as an osmolyte) at 4 °C for 1 s. The osmotic gradient (285 mOSM) drives water efflux, and the consequent reduction in vesicle volume is measured as an increase in the intensity of scattered light (λ = 600 nm). Equation 1 describes the change in volume as a function of membrane permeability (23).

$$dV_{rel}(t)/dt = P_f(S/V_0)v_w(C_i/V_{rel}(t) - C_0) \quad \text{(Eq. 1)}$$

V_{rel}, the vesicular volume relative to the initial volume, is proportional to the intensity of scattered light (24) and is dimensionless. P_f is the osmotic water permeability; S/V_0 is vesicle surface area to initial volume ratio; v_w is the partial molar volume of water (18 cm^3); C_i is the initial intravesicular osmolarity; and C_o is the external osmolarity. Single-exponential time constants (k) were calculated by least squares fit of experimental data. A family of simulated curves was obtained by numerical integration of Equation 1 and fitted to a single exponential. P_f was estimated by iterative comparison of the experimental time constants with the values obtained from the simulation by using MATHCAD software.

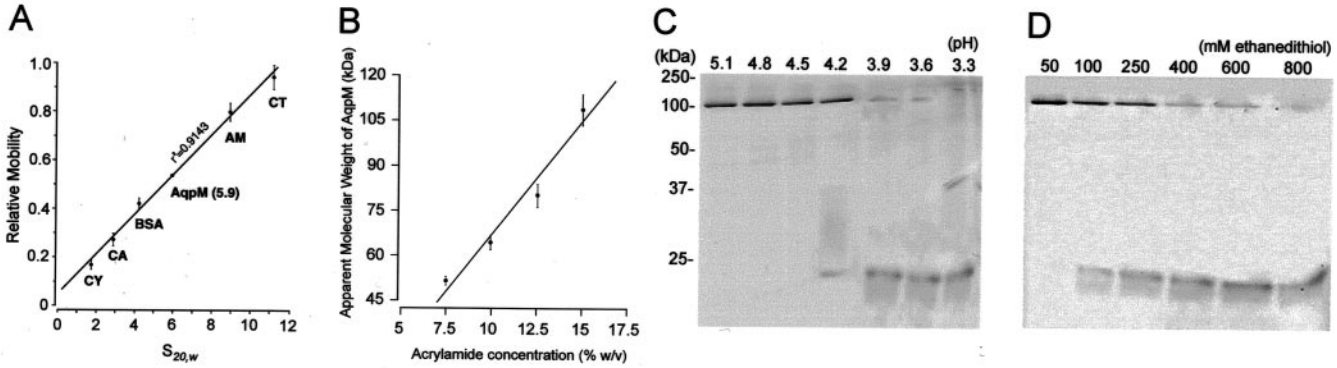

FIG. 3. **Oligomeric state of AqpM.** *A*, solubilized, purified 10-His-AqpM protein was layered on top of a 5–20% continuous sucrose gradient containing 3% OG and centrifuged at 140,000 × *g* for 18 h. 20 fractions were collected and resolved by SDS-PAGE. The sedimentation coefficient ($s_{20,w}$) of AqpM was determined by comparison with the following standards: *CY*, cytochrome *c* (1.8); *CA*, carbonic anhydrase (2.9); *BSA*, bovine serum albumin (4.3); *AM*, β-amylase (8.9); and *CT*, catalase (11.2). All values are mean ± S.E. *B*, purified 10-His-AqpM protein was resolved in SDS-PAGE with different concentrations of acrylamide revealing apparent sizes: ~48 kDa in 7.5% acrylamide, ~68 kDa in 10% acrylamide, ~82 kDa in 12.5% acrylamide, and ~110 kDa in 15% acrylamide. *C*, purified 10-His-AqpM protein was incubated at room temperature in 100 μl of gel loading buffer at pH values from 3.3 to 5.4 for 10 min. Samples were visualized with 15% SDS-PAGE. The 10-His-AqpM tetramer dissociated into monomers at pH <4.2. *D*, purified 10-His-AqpM protein was incubated at room temperature in 100 μl of gel loading buffer (pH 6.8) containing 50–800 mM ethanedithiol for 1 h.

To determine permeability to glycerol and urea, proteoliposomes were equilibrated in assay buffer supplemented with glycerol or urea (~570 mosM). The suspensions were then rapidly mixed with a solution in which osmolarity was compensated by a nonpermeant solute (sucrose). Glycerol and urea permeabilities were measured at 37 °C for 2–4 s under similar conditions as above. The external concentration of permeant solute is reduced by half (285 mosM) without a change in osmolarity, driving the efflux of the permeant osmolyte and generating an outwardly oriented osmotic gradient. Water efflux causes a reduction in volume and an increase in the intensity of scattered light.

To investigate whether AqpM was sensitive to $HgCl_2$, proteoliposomes were incubated with 0.1 mM $HgCl_2$ for 30 min prior to assay; to test reversibility, 5 mM β-mercaptoethanol was incubated for an additional 30 min prior to assay. To determine the thermal stability of AqpM, the proteoliposomes were incubated at temperatures from 30 to 100 °C for 15 min and gradually returned to room temperature prior to permeability assays. For Arrhenius activation energies, water transport permeability measurements were undertaken at temperatures from 4 to 37 °C.

Computer Modeling of AqpM Structure—A tetrameric derivative of the 2.2 Å x-ray diffraction structure of bovine aquaporin-1 (Protein Data Bank code 1J4N) (17) was used as the template. By using data from multiple sequence alignment, the amino acid sequence of AqpM was manually threaded through the template in Swiss Protein Database Viewer (25). The optimal tertiary structure was computed by SWISS-MODEL. Figures were generated with VMD (26) and Raster3D (27).

RESULTS

Mercury-sensitive Water Channel—To evaluate the presence of a water channel in archaeon, *M. marburgensis* cells in exponential growth phase were subjected to hyperosmotic shock and visualized by transmission electron microscopy. Before treatment, cells appeared turgid (Fig. 1*A*). When exposed to hyperosmotic shock with 1 M mannitol, the cells showed retraction of the cytoplasm forming plasmolytic spaces (Fig. 1*B*). Minimal shrinkage was observed in *M. marburgensis* cells pretreated with $HgCl_2$ (Fig. 1*C*), suggesting the functional expression of a water channel that can mediate osmotically driven water flux in this organism. A similar phenomenon was observed in wild-type *E. coli* but not in an AqpZ-null mutant (28).

Phylogenetic Analyses of a Candidate Aquaporin—We recently identified a single aquaporin-like sequence, *aqpM*, in the genome of *M. marburgensis* (19). The deduced amino acid sequence of AqpM was 71 and 50% identical to two candidate aquaporin sequences from other Archaea (*Archaeglobus fulgidus* and *Methanosarcina barkeri*) and 30–36% identical (with gaps) to sequences from eubacteria, yeast, plants, and mammals. Multiple alignments revealed residues that are highly conserved in each of the transmembrane domains as well as the functionally important loops B and E (Fig. 2*A*). Compared with other homologs, the archaeal sequences have a relatively long loop A between TM1 and TM2. Information from the crystal structure of GlpF and hydropathy analysis provided a framework for predicting the membrane topology of AqpM (Fig. 2*B*). We constructed a tree with the neighbor-joining method of phylogenetic inference (29), using sequences from aquaporin homologs that have been functionally characterized (2, 7, 11, 30–39). The phylogenetic tree did not distinguish whether AqpM is an aquaporin or an aquaglyceroporin (Fig. 2*C*). In particular, the residues surrounding the narrowest region of the pore (Ile-187 and Ser-196) do not conform to the corresponding residues in either aquaporins (His-180 and Cys-189 in hAQP1) or aquaglyceroporins (Gly-191 and Phe-200 in GlpF). P2–P5 residues, which distinguish eukaryotic and eubacterial aquaporins from aquaglyceroporins, (4) did not provide clear assignment for AqpM. The P2–P5 residues of AqpM (Thr-203, Tyr-207, Tyr-221, and Val-222) conform with only one residue in the aquaporins (Ser, Ala, Phe/Tyr, and Try) but with none in the aquaglyceroporins (Asp, Arg/Lys, Pro, and Ile/Leu).

Expression and Purification of AqpM—Xenopus laevis oocytes injected with 5 ng of *aqpM* cRNA failed to demonstrate increased water, glycerol, or urea permeabilities (data not shown) as shown for other aquaporins (37). Presumably this reflects failure of eukaryotic oocytes to express an archaeal membrane protein, so we attempted protein expression in bacteria for reconstitution into proteoliposomes. The AqpM protein was predicted to contain only short N- and C-terminal cytoplasmic domains, so the DNA was cloned into the pTrc10HisAqpZ plasmid (8) encoding a polypeptide with a 21-residue extension with 10 consecutive histidine residues at the N terminus of AqpM (10-His-AqpM). *E. coli* cells transformed with pTrc10HisAqpM grew normally in LB-ampicillin medium. Addition of 1 mM isopropyl-β-D-thiogalactoside arrested growth but did not prevent protein expression. In our case, 1 liter of culture typically yielded 3–5 mg of purified protein.

Oligomeric State of AqpM—The purified 10-His-AqpM protein and standard proteins were separately loaded on sucrose gradients. The apparent sedimentation coefficient for the peak fraction, ~5.9 S, was determined by comparing mobilities of 10-His-AqpM to standards ranging from 1.8 to 11.2 S (Fig. 3*A*). The value for OG-solubilized 10-His-AqpM was slightly above the values obtained for DM-solubilized AqpZ (8) and OG-solu-

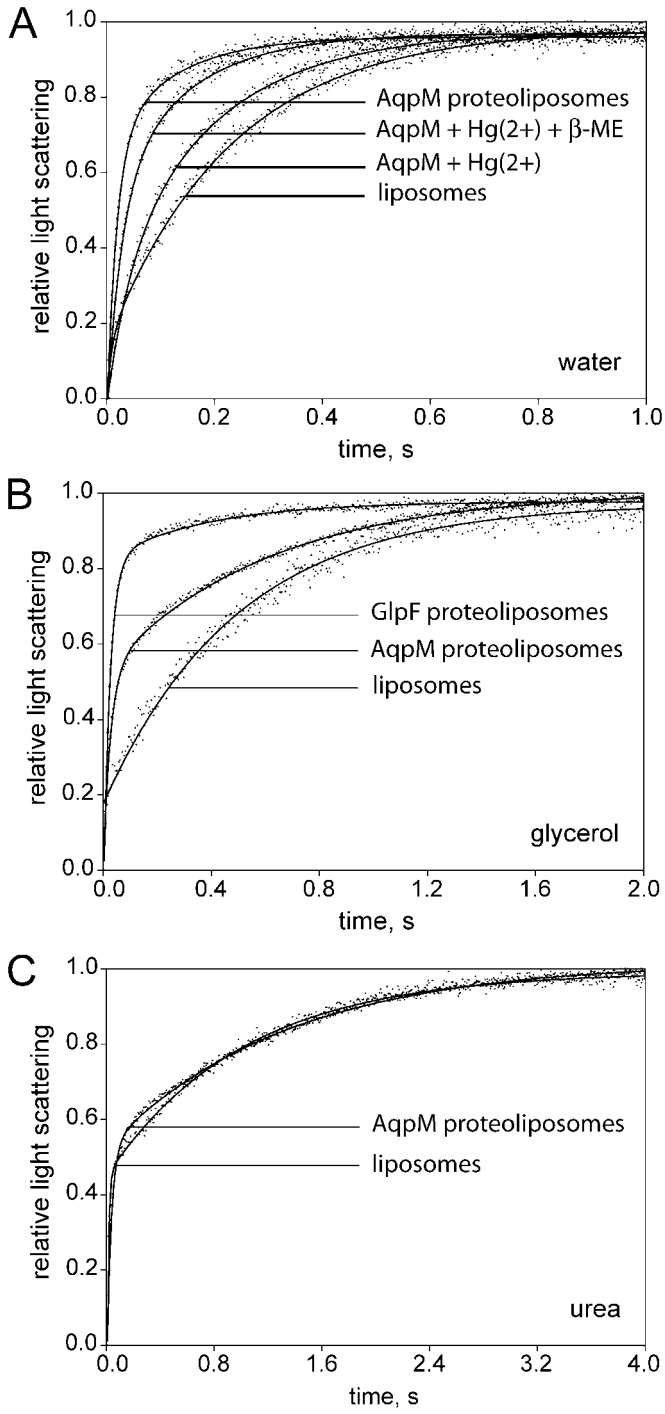

FIG. 4. **Water, glycerol, and urea permeabilities of reconstituted AqpM.** *A*, proteoliposomes reconstituted with purified 10-His-AqpM or control liposomes were abruptly mixed at 4 °C with a similar volume of hyperosmolar solution (reconstitution buffer + 570 mosM sucrose). The increase in light scattering concomitant with a reduction in vesicular volume due to water efflux was monitored in a stopped-flow apparatus for 1 s. The collected data were normalized between zero and unity and fitted to an exponential rise to the maximal value curve. Indicated proteoliposomes were pretreated at room temperature with 0.1 mM $HgCl_2$ for 30 min or pretreated with $HgCl_2$ followed by incubation upon addition of 5 mM β-mercaptoethanol (*β-ME*) for an additional 30 min. Osmotic water permeabilities constants were calculated as follows: P_f(liposomes) = 12 ± 0.7 $\mu m \cdot s^{-1}$, P_f(AqpM proteoliposomes) = 57 ± 4 $\mu m \cdot s^{-1}$, P_f(AqpM + Hg^{2+}) = 17 ± 1.3 $\mu m \cdot s^{-1}$, P_f(AqpM + Hg^{2+} + β-mercaptoethanol) = 33 ± 4 $\mu m \cdot s^{-1}$. All values are mean ± S.D. *B* and *C*, control liposomes or proteoliposomes reconstituted with 10-His-AqpM or GlpF were equilibrated at 37 °C with reconstitution buffer + 570 mosM glycerol or urea for 1 h. These were then abruptly mixed at 37 °C with a similar volume of iso-osmolar solution containing impermeant solutes (reconstitution buffer + 570 mosM sucrose). The increase in light scattering concomitant with a reduction in vesicular volume due to solute and water efflux was monitored in a stopped-flow apparatus for 2–4 s, and the collected data were normalized to fit between zero and unity. Due to a lack of fit to single-order exponential rise to maximal value curves, solute permeability coefficients could not be correctly calculated for AqpM proteoliposomes; the data were fitted to double-exponential rise to maximal curves for visual clarity.

bilized AQP1 (40), which are known to be tetramers.

When visualized by silver staining, the purified 10-His-AqpM protein migrated as a single molecular species of ~110 kDa in 15% acrylamide SDS-PAGE slabs. To evaluate the molecular mass of the ~110-kDa species, the electrophoretic behavior in SDS-PAGE was investigated at different concentrations of acrylamide. A linear relationship was observed between the apparent molecular mass and the acrylamide concentration (Fig. 3*B*), with faster mobility in gels of lower polymer content. This aberrant electrophoretic behavior is characteristic of aquaporins (41). Together, the sedimentation and electrophoretic studies suggest that 10-His-AqpM exists as a tetramer when solubilized either in mild detergents, such as OG, or strong detergents, such as SDS, which usually unfolds and dissociates protein subunits.

Dissociation of the tetramer was attempted under several different conditions. Incubation of the samples with chaotropic (8 M urea or guanidinium chloride) or hydrophilic reducing agents (500 mM β-mercaptoethanol or 1000 mM dithiothreitol) did not cause any dissociation of 10-His-AqpM, even after 1 week (data not shown). Incubation at pH <4.0 (Fig. 3*C*) or with the reducing agent ethanedithiol at a concentration of 600 mM (Fig. 3*D*) led to almost complete dissociation of 10-His-AqpM to a monomer with the predicted size of ~24 kDa.

Permeabilities of Reconstituted AqpM—AqpM proteoliposomes were prepared by dilution with *E. coli* lipids and 10-His-AqpM at a lipid-to-protein ratio of 75:1. AqpM proteoliposomes and control liposomes were abruptly transferred to an outwardly directed osmotic gradient, and the changes recorded in light scattering were measured at λ_{em} = 600 nm (Fig. 4*A*). AqpM proteoliposomes exhibited a moderately high osmotic water permeability of 57 ± 4 $\mu m \cdot s^{-1}$, whereas control liposomes yielded much lower permeability, 12 ± 0.7 $\mu m \cdot s^{-1}$. The permeability of AqpM proteoliposomes was 90% inhibited by treatment with 0.1 mM $HgCl_2$. However, the inhibition was partially reversed with 5 mM β-mercaptoethanol. The Arrhenius activation energy was calculated from measurements performed at various temperatures from 4 to 37 °C, yielding a value ($E_{a(water)}$ = 2.67 kcal/mol) consistent with water transport through a channel as opposed to diffusion across the lipid bilayer as seen in control liposomes ($E_{a(water)}$ = 12.9 kcal/mol).

AqpM proteoliposomes consistently exhibited a transient initial phase of glycerol permeability that was above the permeability of control liposomes but was much less than the sustained glycerol permeability of proteoliposomes reconstituted with the *E. coli* glycerol facilitator, GlpF (Fig. 4*B*). AqpM proteoliposomes did not exhibit significant urea permeability above that of control liposomes (Fig. 4*C*).

Thermostability of AqpM—Because *M. marburgensis* is a thermophile, AqpM was expected to be stable at higher temperatures. We attempted to measured water permeabilities of AqpM proteoliposomes at elevated temperatures, but above 37 °C the control liposomes became leaky, preventing accurate measurements (data not shown). Thus, we pretreated AqpM proteoliposomes at temperatures up to 100 °C for 15 min and then performed stopped-flow measurements at room temperature. AqpM proteoliposomes retained most water permeability after pretreatments up to 80 °C but were inactive after 90 °C

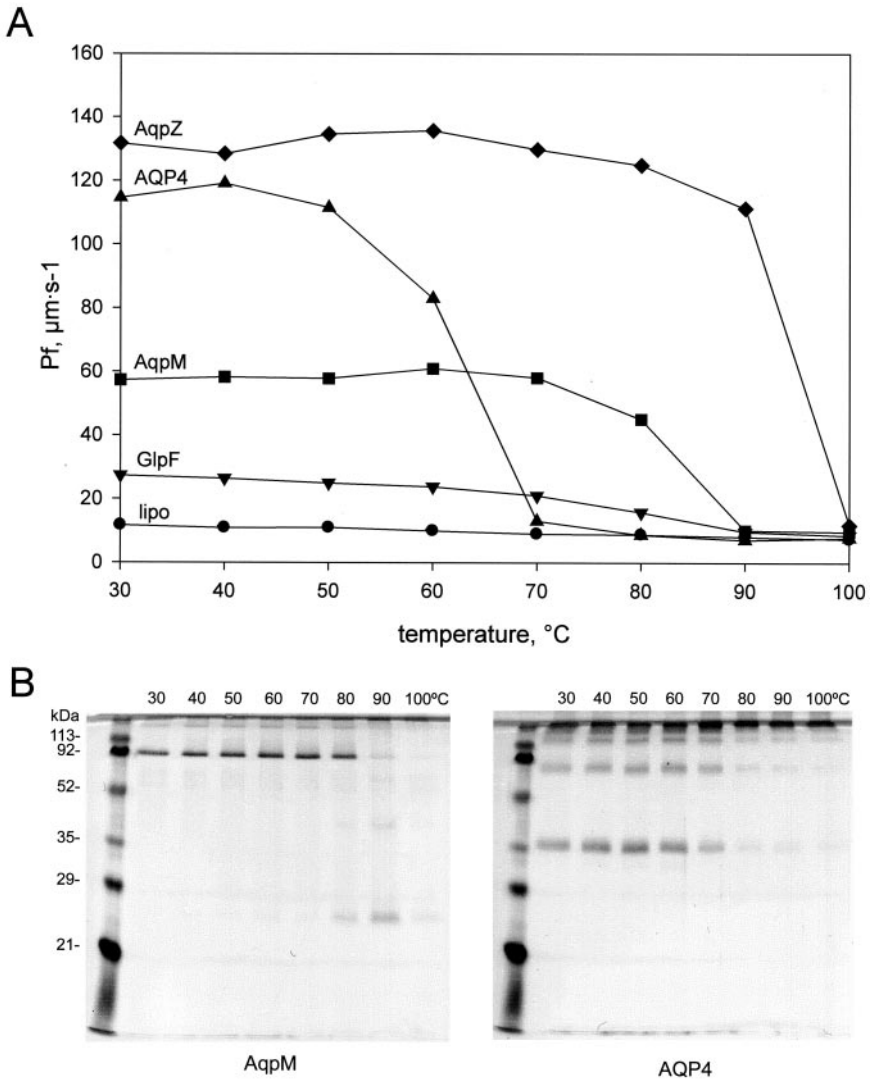

FIG. 5. **Thermostability of reconstituted aquaporins.** *A*, proteoliposomes reconstituted with 10-His-AqpM, AqpZ, GlpF, or rat AQP4 and control liposomes (*lipo*) were incubated for 15 min at temperatures from 30 to 100 °C and then gradually cooled to room temperature. Water permeabilities were measured and calculated as described. *B*, silver-stained 14% SDS-PAGE gels of 10-His-AqpM and rat AQP4 proteoliposomes treated at different temperatures from 30 to 100 °C.

(Fig. 5*A*). In contrast, rat AQP4 lost most activity after pretreatments at 70 °C. Although *E. coli* is not a thermophile, AqpZ proteoliposomes retained most activity after pretreatments at 90 °C but were inactive after 100 °C. Silver-stained SDS-PAGE gels of heat-treated AqpM proteoliposomes and rat AQP4 proteoliposomes revealed evidence of protein aggregation at the top of the lanes after pretreatments at the inactivating temperatures (Fig. 5*B*).

DISCUSSION

First isolated from sewage sludge, *M. marburgensis* is a methanogenic archaeon that grows optimally in an anaerobic environment at 65 °C and utilizes carbon dioxide as a sole carbon source (1). Hypertonic treatment of living *M. marburgensis* cells revealed mercury-sensitive water permeability that led to the archaeal aquaporin homolog, AqpM. Members of the major intrinsic protein (MIP) family including water channels (aquaporins) and glycerol transporters (aquaglyceroporins) have been identified in diverse organisms including vertebrates, invertebrates, plants, and microorganisms (42). This study represents the biophysical characterization of a homolog from the third kingdom of life, Archaea.

The question of why unicellular organisms express aquaporins remains open. The channel formed by the *E. coli* water channel AqpZ has been shown to mediate large water fluxes in response to sudden changes in extracellular osmolarity (28). A role in cell proliferation in hypotonic environments was proposed (43), but adverse effects were not identified after disruption of *aqpZ* (10). There is evidence that the two aquaporin genes in *S. cerevisiae*, *AQY1* and *AQY2*, may confer freeze tolerance in industrial yeast strains (44), although both were found to contain multiple mutations causing loss of function without clearly adverse effects to the laboratory strains of this organism (32, 45).

Investigators (4) studying osmoadaptation in Archaea hypothesized the existence of water channels to survive hypertonic shock following accumulation of osmolytes. In this study, we confirmed the existence of a water channel in one archaeal species by *in vivo* and *in vitro* water permeability analyses. The osmotic water permeability of proteoliposomes reconstituted with purified polyhistidine-tagged AqpM was severalfold above control liposomes but below proteoliposomes containing *E. coli* AqpZ. Moreover, AqpM proteoliposomes exhibited a transient but reproducible increase in the initial glycerol flux, although the overall glycerol permeation was much lower than proteoliposomes containing the *E. coli* glycerol facilitator, GlpF. Our studies indicate that AqpM is a primitive member of the large MIP family, because it functions as a moderate water channel but a very poor glycerol transporter, so we can only speculate about its biological function in the host organism.

Growth of Archaea in severe environments is made possible by special plasma membranes composed of lipids that differ markedly in structure and physicochemical properties from the glycerolipids of eubacterial and eukaryotic cell membranes. For

Archaea to maintain water balance while growing in extreme pH environments (46), tight control of proton and water fluxes is required (47). Unlike glycerolipids, which become highly permeable to water and protons at elevated temperatures, the rigid structures of archaeal lipids have particularly low permeability to water, protons, and other ions even at high temperatures (48). AqpM was found to retain its tertiary structure in SDS and had greater thermostability than AQP4, a mammalian homolog (Figs. 3 and 5). Interestingly, AqpZ from *E. coli* also had high thermostability. Comparison of the amino acid sequences of aquaporins from mesophilic species with that of thermophilic AqpM showed considerable amino acid sequence identity (Fig. 2*A*) and did not reveal an obvious explanation for the high thermostability. The existence of AqpM provides a mechanism for thermophilic Archaea like *M. marburgensis* to increase the water permeability of their plasma membranes while remaining impermeable to protons.

Statistical sequence analyses had identified previously residues, P2–P5, that distinguish water channels from glycerol transporters (5), but the sequence of AqpM is ambiguous. Residues lining the narrowest region of the pore and the P2–P5 do not completely conform to aquaporins or aquaglyceroporins (Fig. 2, *A* and *B*). The lower water permeability but transient glycerol permeability observed in AqpM proteoliposomes suggests an intermediate function. Some eubacteria such as *E. coli* have been shown to possess both water-specific and glycerol-specific aquaporins, but the *Methanothermobacter* genome contains only a single homologous sequence (49). It is heuristically appealing to regard the AqpM sequence as representative of a progenitor sequence of the more functionally differentiated channel proteins found in other kingdoms of life (50).

The high permeation selectivities of mammalian water channel protein AQP1 and *E. coli* glycerol facilitator GlpF have been explained with atomic resolution structures (17). A hydrophilic pore-lining residue (His-180 in human AQP1) is critical for rapid water transport but hinders passage of glycerol (17). AqpM has an aliphatic residue at this position (Ile-187). In the three-dimensional structure of GlpF, this position is occupied by a perpendicularly oriented residue (Phe-200) that contributes to glycerol permeation (14). Because of these and other differences, GlpF has a pore size that is 1 Å wider than that of AQP1 at the point of narrowest constriction. A computer-generated model predicts that AqpM has a pore size intermediate between that of AQP1 and GlpF (Fig. 6). The diameter and hydrophobicity of this aperture may be critical in providing structural clues that determine the channel selectivities.

Mammalian water channel proteins were recognized in early studies by their reversible inhibition by mercurials (51). This may result from occlusion of the pore by covalent attachment of Hg^{2+} to the free sulfhydryl of a cysteine within the pore (Fig. 6, Cys-189 in AQP1) (52). Many aquaporins, including AqpZ, are not inhibited by mercurials (52), so it was surprising to find that the water permeability of AqpM was reversibly blocked by treatment with $HgCl_2$ (Fig. 4*A*). Curiously, the mercury-inhibitable cysteine in AqpM does not reside proximal to the second NPA motif in loop E, as in AQP1 and some other mammalian aquaporins (52), but in the corresponding position in loop B (Fig. 2*B*). By site-directed mutagenesis of AQP1, this position was shown to be structurally and functionally equivalent, predicting the unique "hourglass" structure for AQP1 and other aquaporins (38).

Although disputed (53), several studies (54–56) suggested that some aquaporins are permeated by carbon dioxide. Carbon dioxide entry into cyanobacteria (57) and photosynthetic activity (58) were drastically inhibited by *p*-chloromercuriphenylsulfonic acid and recovered with β-mercaptoethanol. *M. marburgensis* is an absolute anaerobe and utilizes carbon dioxide as a sole carbon source (20). When AqpM was expressed in *E. coli* strain SK46 containing disruptions of both *aqpZ* and *glpF*, $^{14}CO_2$ permeability through the bacterial membrane was increased above control *E. coli*.[3] Thus, AqpM may provide a model molecule for elucidation of carbon dioxide permeation through aquaporins.

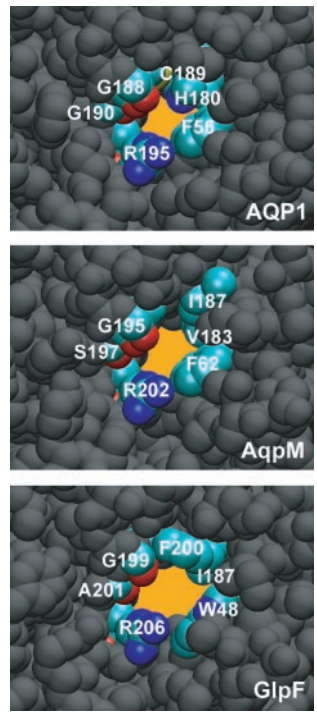

FIG. 6. **Computer modeling of AqpM.** These figures depict the transmembrane sections of human AQP1, *M. marburgensis* AqpM, and *E. coli* GlpF, as seen from the extracellular face through the axis of the pore. AQP1 (human residue numbers based upon bovine AQP1) and *E. coli* GlpF are from atomic resolution x-ray diffraction coordinates (Protein Data Bank codes 1J4N and 1FX8, respectively). AqpM is computer modeled, based on the bovine AQP1 structure. All atoms are shown as van der Waals space-filling spheres; critical pore-lining residues are labeled and highlighted in color (carbon atoms are *turquoise*, oxygen atoms are *red*, nitrogen atoms are *blue*, and sulfur atoms are *yellow*). The pore is colored *bright orange* for clarity.

Aquaporins and aquaglyceroporins form the major intrinsic protein, MIP, family that is believed to date back 2.5–3 billion years in evolutionary time (42). Recognition of an aquaporin in an archaeon suggests an even earlier origin, although it is possible that the gene was transferred horizontally from other microorganisms (59, 60). From our phylogenetic analysis, we believe that eukaryotic members of the MIP family evolved from two basal lineages: AqpZ-like water channels and GlpF-like glycerol facilitators. These divergent lineages may have originated from an AqpM-like sequence, which appears to be intermediate in sequence between the water-selective aquaporins and the aquaglyceroporins (50). The current abundance of sequence data together with new functional information warrants reinvestigation of the phylogenetic origins of the ubiquitous family of water channel proteins.

Acknowledgments—We thank Prof. Reiner Hedderich, Max-Planck-Institut fuer Terrestrische Mikrobiologie, Germany, for kindly providing genomic DNA and *M. marburgensis* and Prof. Giuseppe Calamita, Dipartimento di Fisiologia Generale e Ambientale Università degli Studi di Bari via Amendola, 165/A 70126 Bari, Italy, for critical discussions. We also thank M. Odara and K. Nakahara and M. Sugawara and M. Goto for constant encouragement and technical help.

[3] X. Ding, unpublished results.

REFERENCES

1. Wasserfallen, A., Nolling, J., Pfister, P., Reeve, J., and Conway, D. M. (2000) *Int. J. Syst. Evol. Microbiol.* **50,** 43–53
2. Preston, G. M., Carroll, T. P., Guggino, W. B., and Agre, P. (1992) *Science* **256,** 385–387
3. Agre, P., King, L. S., Yasui, M., Guggino, W. B., Ottersen, O. P., Fujiyoshi, Y., Engel, A., and Nielsen, S. (2002) *J. Physiol. (Lond.)* **542,** 3–16
4. Roberts, M. F. (2000) *Front. Biosci.* **5,** D796–D812
5. Froger, A., Tallur, B., Thomas, D., and Delamarche, C. (1998) *Protein Sci.* **7,** 1458–1468
6. Lagree, V., Froger, A., Deschamps, S., Hubert, J. F., Delamarche, C., Bonnec, G., Thomas, D., Gouranton, J., and Pellerin, I. (1999) *J. Biol. Chem.* **274,** 6817–6819
7. Calamita, G., Bishai, W. R., Preston, G. M., Guggino, W. B., and Agre, P. (1995) *J. Biol. Chem.* **270,** 29063–29066
8. Borgnia, M. J., Kozono, D., Calamita, G., Maloney, P. C., and Agre, P. (1999) *J. Mol. Biol.* **291,** 1169–1179
9. Csonka, L. N., and Hanson, A. D. (1991) *Annu. Rev. Microbiol.* **45,** 569–606
10. Soupene, E., King, N., Lee, H., and Kustu, S. (2002) *J. Bacteriol.* **184,** 4304–4307
11. Heller, K. B., Lin, E. C., and Wilson, T. H. (1980) *J. Bacteriol.* **144,** 274–278
12. Maurel, C., Reizer, J., Schroeder, J. I., Chrispeels, M. J., and Saier, M. H., Jr. (1994) *J. Biol. Chem.* **269,** 11869–11872
13. Borgnia, M. J., and Agre, P. (2001) *Proc. Natl. Acad. Sci. U. S. A.* **98,** 2888–2893
14. Fu, D., Libson, A., Miercke, L. J., Weitzman, C., Nollert, P., Krucinski, J., and Stroud, R. M. (2000) *Science* **290,** 481–486
15. Murata, K., Mitsuoka, K., Hirai, T., Walz, T., Agre, P., Heymann, J. B., Engel, A., and Fujiyoshi, Y. (2000) *Nature* **407,** 599–605
16. de Groot, B. L., Engel, A., and Grubmuller, H. (2001) *FEBS Lett.* **504,** 206–211
17. Sui, H., Han, B. G., Lee, J. K., Walian, P., and Jap, B. K. (2001) *Nature* **414,** 872–878
18. Stetter, K. O., Huber, R., Blochl, E., Kurr, M., Eden, R. D., Fielder, M., Cash, H., and Vance, I. (1993) *Nature* **365,** 743–745
19. Ding, X., and Kitagawa, Y. (2001) *J. Biosci. Bioeng.* **92,** 488–491
20. Schonheit, P., Moll, J., and Thauer, R. K. (1979) *Arch. Microbiol.* **123,** 105–107
21. Saparov, S. M., Kozono, D., Rothe, U., Agre, P., and Pohl, P. (2001) *J. Biol. Chem.* **276,** 31515–31520
22. Schaffner, W., and Weissmann, C. (1973) *Anal. Biochem.* **56,** 502–514
23. Zeidel, M. L., Ambudkar, S. V., Smith, B. L., and Agre, P. (1992) *Biochemistry* **31,** 7436–7440
24. Illsley, N. P., and Verkman, A. S. (1986) *J. Membr. Biol.* **94,** 267–278
25. Guex, N., and Peitsch, M. C. (1997) *Electrophoresis* **18,** 2714–2723
26. Humphrey, W., Dalke, A., and Schulten, K. (1996) *J. Mol. Graphics* **14,** 33–38
27. Merritt, E. A., and Bacon, D. J. (1997) *Methods Enzymol.* **277,** 505–524
28. Delamarche, C., Thomas, D., Rolland, J. P., Froger, A., Gouranton, J., Svelto, M., Agre, P., and Calamita, G. (1999) *J. Bacteriol.* **181,** 4193–4197
29. Saitou, N., and Nei, M. (1987) *Mol. Biol. Evol.* **4,** 406–425
30. Rodriguez, M. C., Froger, A., Rolland, J. P., Thomas, D., Aguero, J., Delamarche, C., and Garcia-Lobo, J. M. (2000) *Microbiology* **146,** 3251–3257
31. Froger, A., Rolland, J. P., Bron, P., Lagree, V., Le Caherec, F., Deschamps, S., Hubert, J. F., Pellerin, I., Thomas, D., and Delamarche, C. (2001) *Microbiology* **147,** 1129–1135
32. Bonhivers, M., Carbrey, J. M., Gould, S. J., and Agre, P. (1998) *J. Biol. Chem.* **273,** 27565–27572
33. Luyten, K., Albertyn, J., Skibbe, W. F., Prior, B. A., Ramos, J., Thevelein, J. M., and Hohmann, S. (1995) *EMBO J.* **14,** 1360–1371
34. Maurel, C., Reizer, J., Schroeder, J. I., and Chrispeels, M. J. (1993) *EMBO J.* **12,** 2241–2247
35. Kammerloher, W., Fischer, U., Piechottka, G. P., and Schaffner, A. R. (1994) *Plant J.* **6,** 187–199
36. Weig, A. R., and Jakob, C. (2000) *FEBS Lett.* **481,** 293–298
37. Ishibashi, K., Sasaki, S., Fushimi, K., Uchida, S., Kuwahara, M., Saito, H., Furukawa, T., Nakajima, K., Yamaguchi, Y., Gojobori, T., and Marumo, F. (1994) *Proc. Natl. Acad. Sci. U. S. A.* **91,** 6269–6273
38. Jung, J. S., Bhat, R. V., Preston, G. M., Guggino, W. B., Baraban, J. M., and Agre, P. (1994) *Proc. Natl. Acad. Sci. U. S. A.* **91,** 13052–13056
39. Ishibashi, K., Kuwahara, M., Kageyama, Y., Tohsaka, A., Marumo, F., and Sasaki, S. (1997) *Biochem. Biophys. Res. Commun.* **237,** 714–718
40. Mathai, J. C., and Agre, P. (1999) *Biochemistry* **38,** 923–928
41. Helenius, A., and Simons, K. (1975) *Biochim. Biophys. Acta* **415,** 1–147
42. Reizer, J., Reizer, A., and Saier, M. H., Jr. (1993) *Crit. Rev. Biochem. Mol. Biol.* **28,** 235–257
43. Calamita, G., Kempf, B., Bonhivers, M., Bishai, W. R., Bremer, E., and Agre, P. (1998) *Proc. Natl. Acad. Sci. U. S. A.* **95,** 3627–3631
44. Tanghe, A., Van Dijck, P., Dumortier, F., Teunissen, A., Hohmann, S., and Thevelein, J. M. (2002) *Appl. Environ. Microbiol.* **68,** 5981–5989
45. Carbrey, J. M., Bonhivers, M., Boeke, J. D., and Agre, P. (2001) *Proc. Natl. Acad. Sci. U. S. A.* **98,** 1000–1005
46. Segerer, A., Neuner, A., Kristjansson, J. K., and Stetter, K. O. (1986) *Int. J. Syst. Bacteriol.* **36,** 559–564
47. van de Vossenberg, J. L., Driessen, A. J., and Konings, W. N. (1998) *Extremophiles* **2,** 163–170
48. Mathai, J. C., Sprott, G. D., and Zeidel, M. L. (2001) *J. Biol. Chem.* **276,** 27266–27271
49. Smith, D. R., Doucette-Stamm, L. A., Deloughery, C., Lee, H., Dubois, J., Aldredge, T., Bashirzadeh, R., Blakely, D., Cook, R., Gilbert, K., Harrison, D., Hoang, L., Keagle, P., Lumm, W., Pothier, B., Qiu, D., Spadafora, R., Vicaire, R., Wang, Y., Wierzbowski, J., Gibson, R., Jiwani, N., Caruso, A., Bush, D., and Reeve, J. N. (1997) *J. Bacteriol.* **179,** 7135–7155
50. Zardoya, R., Ding, X., Kitagawa, Y., and Chrispeels, M. J. (2002) *Proc. Natl. Acad. Sci. U. S. A.* **99,** 14893–14896
51. Macey, R. I., and Farmer, R. E. L. (1970) *Biochim. Biophys. Acta* **211,** 104–106
52. Preston, G. M., Jung, J. S., Guggino, W. B., and Agre, P. (1993) *J. Biol. Chem.* **268,** 17–20
53. Yang, B., Fukuda, N., van Hoek, A., Matthay, M. A., Ma, T., and Verkman, A. S. (2000) *J. Biol. Chem.* **275,** 2686–2692
54. Nakhoul, N. L., Davis, B. A., Romero, M. F., and Boron, W. F. (1998) *Am. J. Physiol.* **274,** C543–C548
55. Prasad, G. V., Coury, L. A., Finn, F., and Zeidel, M. L. (1998) *J. Biol. Chem.* **273,** 33123–33126
56. Sun, X. C., Allen, K. T., Xie, Q., Stamer, W. D., and Bonanno, J. A. (2001) *Investig. Ophthalmol. Vis. Sci.* **42,** 417–423
57. Tchernov, D., Helman, Y., Keren, N., Luz, B., Ohad, I., Reinhold, L., Ogawa, T., and Kaplan, A. (2001) *J. Biol. Chem.* **276,** 23450–23455
58. Allakhverdiev, S. I., Sakamoto, A., Nishiyama, Y., and Murata, N. (2000) *Plant Physiol.* **122,** 1201–1208
59. Nelson, K. E., Clayton, R. A., Gill, S. R., Gwinn, M. L., Dodson, R. J., Haft, D. H., Hickey, E. K., Peterson, J. D., Nelson, W. C., Ketchum, K. A., McDonald, L., Utterback, T. R., Malek, J. A., Linher, K. D., Garrett, M. M., Stewart, A. M., Cotton, M. D., Pratt, M. S., Phillips, C. A., Richardson, D., Heidelberg, J., Sutton, G. G., Fleischmann, R. D., Eisen, J. A., and Fraser, C. M. (1999) *Nature* **399,** 323–329
60. Salzberg, S. L., White, O., Peterson, J., and Eisen, J. A. (2001) *Science* **292,** 1903–1906